Heat and Mass Transfer 37 (2001) 117–123 © Springer-Verlag 2001

Similarity solutions for hydromagnetic simultaneous heat and mass transfer by natural convection from an inclined plate with internal heat generation or absorption

Ali J. Chamkha, Abdul-Rahim A. Khaled

Abstract The problem of coupled heat and mass transfer by natural convection from a semi-infinite inclined flat plate in the presence of an external magnetic field and internal heat generation or absorption effects is formulated. The plate surface has a power-law variation of both wall temperature and concentration and is permeable to allow for possible fluid wall suction or blowing. The resulting governing equations are transformed using a similarity transformation and then solved numerically by an implicit, iterative, finite-difference scheme. Comparisons with previously published work are performed and good agreement is obtained. A parametric study of all involved parameters is conducted and a representative set of numerical results for the velocity and temperature profiles as well as the skin-friction parameter, average Nusselt number, and the average Sherwood number is illustrated graphically to show typical trends of the solutions.

List of symbols

a	Wall temperature or concentration power index
a^*	Coefficient of space-dependent internal heat generation/absorption
b^*	Coefficient of temperature-dependent internal heat absorption
B_0	Magnetic field strength
c_p	Specific heat of the fluid
C	Concentration at any point in the flow field
C_∞	Concentration at the free stream
C_w	Concentration at the wall
D	Mass diffusivity
f	Dimensionless stream function $(f = \psi/(4\upsilon)(\mathrm{Gr}_x/4)^{-1/4})$
f_0	Transformed wall mass transfer coefficient $(f_0 = V_w x(\mathrm{Gr}_x/4)^{-1/4})/(3+a))$
g	Gravitational acceleration
Gr_x	Local Grashof number $(\mathrm{Gr}_x = g\beta_T(T_w - T_\infty)x^3/\upsilon^2)$
h	Average convective heat transfer coefficient
h_m	Average mass transfer coefficient
k	Fluid thermal conductivity
L	Characteristic length of the plate
N	Buoyancy ratio $(N = (C_w - C_\infty)/(T_w - T_\infty))$
M	Square of the Hartmann number $(M = (\sigma B_0^2 x^2)(\mathrm{Gr}_x/4)^{-3/4}/\mu)$
Nu_{avg}	Average Nusselt number $(\mathrm{Nu}_{avg} = hL/k)$
Pr	Prandtl number $(\mathrm{Pr} = \mu c_p/k)$
q'''	Internal heat generation or absorption rate
Sc	Schmidt number $(\mathrm{Sc} = \upsilon/D)$
Sh_{avg}	Average Sherwood number $(\mathrm{Sh}_{avg} = h_m L/D)$
T	Temperature at any point
T_w	Wall temperature
T_∞	Free stream temperature
u	Tangential or x-component of velocity
v	Normal or y-component of velocity
V_w	Wall mass transfer velocity
x	Distance along the plate
y	Distance normal to the plate

Greek symbols

α	Inclination angle from vertical direction
β_C	Concentration expansion coefficient
β_T	Thermal expansion coefficient
ϕ	Dimensionless concentration $(\phi = (C - C_\infty)/(C_w - C_\infty))$
η	Coordinate transformation in terms of x and y $(\eta = y/(x(\mathrm{Gr}_x/4)^{-1/4}))$
μ	Fluid dynamic viscosity
υ	Fluid kinematic viscosity
ψ	Dimensional stream function
θ	Dimensionless temperature $(\theta = (T - T_\infty)/(T_w - T_\infty))$
ρ	Fluid density
σ	Fluid electrical conductivity
τ_w	Wall shear stress

1 Introduction

Coupled heat and mass transfer finds applications in a variety of engineering processes such as migration of moisture in heat exchanger devices, petroleum reservoirs, filtration, chemical catalytic reactors and processes, nuclear waste repositories, spreading of chemical pollutants in plants, diffusion of medicine in blood veins and extraction of geothermal energy. In addition, coupled heat and mass transfer can interpret certain natural phenomena such as ocean currents driven by differential heating and act as freight trains for salt as mentioned by Bejan (1993), and the role of factories waste gas diffusion in a differential heating circulated air. Early studies which considered coupled heat and mass transfer include the works of Gebhart and Pera (1971) on vertical plates, Pera and

Received on 26 October 1998

Ali J. Chamkha (✉), Abdul-Rahim A. Khaled
Department of Mechanical and Industrial Engineering
Kuwait University
Safat, 13060 Kuwait

Gebhart (1972) and Chen and Yuh (1980) on inclined plates.

Lately, hydromagnetic flow and heat transfer problems have become more important industrially. As a result, some research have been carried out on the effects of electrically-conducting fluids such as liquid metals, water and others in the presence of magnetic field on the flow and heat transfer aspects (e.g., Michiyoshi et al., 1976; Gray, 1979, Fumizawa, 1980; Vajravelu and Nayfeh, 1992; Chamkha, 1997a).

In many situations, there may be appreciable temperature difference between the surface and the ambient fluid. This necessitates the consideration of temperature-dependent heat sources or sinks which may exert strong influence on the heat transfer characteristics (Vajravelu and Nayfeh, 1992). The study of heat generation or absorption effects in moving fluids is important in view of several physical problems such as fluids undergoing exothermic or endothermic chemical reactions (see Vajravelu and Hadjinicolaou, 1993 and Vajravelu and Nayfeh, 1992). In addition, natural convection with heat generation can be applied to combustion modeling (Westphal et al., 1994). Although, exact modeling of the internal heat generation or absorption is quite difficult, some simple mathematical models can express its average behavior for most physical situations. Heat generation or absorption has been assumed to be constant, space-dependent or temperature dependent. Sparrow and Cess (1961) have considered temperature-dependent heat absorption in their work on steady stagnation point flow and heat transfer. Moalem (1976) has studied the effect of temperature-dependent heat sources taking place in electrical heating on the heat transfer within a porous medium. Vajravelu and Nayfeh (1992) have reported on the hydromagnetic convection at a cone and a wedge in the presence of temperature-dependent heat generation or absorption effects. Recently, Chamkha (1997b) has considered linear variation with temperature heat sources or sinks in his work on mixed convection in a channel filled with a porous medium. Finally, Crepeau and Clarksean (1997) have used a space-dependent exponentially decaying heat generation or absorption model in their work on flow and heat transfer from a vertical plate.

The objective of this paper is to consider simultaneous heat and mass transfer of electrically-conducting fluid by natural convection from an inclined plate in the presence of mass blowing or suction, magnetic field effects and space-dependent or temperature-dependent heat generation or absorption effects. This will be done for power-law variations of both the wall temperature and concentration.

2 Problem formulation

Consider steady, laminar, hydromagnetic coupled heat and mass transfer by natural convection flow along a semi-infinite permeable inclined plate. Both the wall temperature and concentration vary with the distance along the plate according to a power-law model and they are always greater than their uniform ambient values existing far from the plate surface. A magnetic field of variable strength B_0 is applied in the y-direction which is normal to the flow direction. Fluid suction or blowing is imposed at the plate surface. The fluid is assumed to be Newtonian, electrically conducting, heat generating or absorbing and has constant properties except the density in the buoyancy term of the balance of linear momentum equation. The magnetic Reynolds number is assumed to be small so that the induced magnetic field can be neglected. In addition, there is no applied electric field and both of the Hall effect and viscous dissipation are neglected. Invoking the Boussinesq and boundary-layer approximations, the governing equations for this problem can be written as

$$\frac{\partial u}{\partial x}+\frac{\partial v}{\partial y}=0 \tag{1}$$

$$u\frac{\partial u}{\partial x}+v\frac{\partial u}{\partial y}=\upsilon\frac{\partial^2 u}{\partial y^2}+\beta_T g(T-T_\infty)\cos\alpha + \beta_C g(C-C_\infty)\cos\alpha-\frac{\sigma B_0^2}{\rho}u \tag{2}$$

$$\rho c_p\left(u\frac{\partial T}{\partial x}+v\frac{\partial T}{\partial y}\right)=k\frac{\partial^2 T}{\partial y^2}+q''' \tag{3}$$

$$u\frac{\partial C}{\partial x}+v\frac{\partial C}{\partial y}=D\frac{\partial^2 C}{\partial y^2} \tag{4}$$

where u, v, T and C are the fluid x-component of velocity, y-component of velocity, temperature, and concentration, respectively. The symbols ρ, υ, c_p, β_T, and β_C correspond to the fluid density, kinematic viscosity, specific heat at constant pressure, coefficient of concentration expansion, respectively. The symbols σ, q''', D, g and B_0 correspond to the fluid electrical conductivity, rate of internal heat generation (>0) or absorption (<0) coefficient, mass diffusivity, gravitational acceleration and magnetic induction, respectively. Also, the symbols k, α, T_∞ and C_∞ stand for the fluid thermal conductivity, inclination angle from the vertical direction and the ambient fluid temperature and concentration, respectively.

The internal heat generation or absorption term q''' is modeled according to the following equation:

$$q'''=\left(\frac{k\mathrm{Gr}_x}{4x^2}\right)(a^*(T_w-T_\infty)\,e^{(-\eta)}+(b^*(T-T_\infty))) \tag{5}$$

In Eq. (5), the first term represents the dependence of the internal heat generation or absorption on the space coordinates while the last term represents its dependence on the temperature. Note that when both $a^*>0$ and $b^*>0$, the case will be internal heat generation while it will be internal heat absorption when both a^* and b^* are less than zero.

The above problem is solved, subject to the following boundary conditions:

$$\begin{aligned} &u(x,0)=0,\ v(x,0)=-V_w,\ T(x,0)=T_w,\ C(x,0)=C_w\\ &u(x,\infty)=0,\ \ T(x,\infty)=T_\infty,\ \ C(x,\infty)=C_\infty \end{aligned} \tag{6}$$

where V_w, T_w and C_w are variables representing the suction (>0) or injection (<0) velocity and the fluid temperature and concentration at the plate, respectively.

Both the wall temperature and concentration are assumed to have power-law variation forms as shown by the following equations:

$$T_w = T_\infty + c_1 x^a, \quad C_w = C_\infty + c_2 x^a \tag{7}$$

where c_1 and c_2 are constants and "a" is the power index of the wall temperature and concentration.

Introducing the similarity variables employed earlier by Jaluria (1980) and later by Crepeau and Clarksean (1997) gives

$$\eta = \frac{y}{x}\left(\frac{\mathrm{Gr}_x}{4}\right)^{1/4}, \quad \psi(x,y) = 4\upsilon f(\eta)\left(\frac{\mathrm{Gr}_x}{4}\right)^{1/4}, \\ \theta(\eta) = \frac{T - T_\infty}{T_w - T_\infty}, \quad \phi(\eta) = \frac{C - C_\infty}{C_w - C_\infty} \tag{8}$$

where $\mathrm{Gr}_x = g\beta_T(T_w - T_\infty)x^3/\upsilon^2$ is the local Grashof number.

Substituting Eqs. (5) and (8) into Eqs. (2)–(4) produces the following similarity equations:

$$f''' + (3+a)ff'' - 2(1+a)f'^2 + \theta\cos\alpha + N\phi\cos\alpha - Mf' = 0 \tag{9}$$

$$\theta'' + (3+a)\,\mathrm{Pr}\, f\theta' + a^* e^{(-\eta)} + b^*\theta - 4a\,\mathrm{Pr}\,\theta = 0 \tag{10}$$

$$\phi'' + (3+a)\mathrm{Sc}\, f\phi' - 4a\,\mathrm{Pr}\,\phi = 0 \tag{11}$$

where a prime denotes ordinary differentiation with respect to η and

$$\mathrm{Pr} = \frac{\mu c_p}{k}, \quad \mathrm{Sc} = \frac{\upsilon}{D}, \\ M = \frac{\sigma B_0^2 x^2}{\mu}\left(\frac{\mathrm{Gr}_x}{4}\right)^{-3/4}, \quad N = \frac{\beta_C(C_w - C_\infty)}{\beta_T(T_w - T_\infty)} \tag{12}$$

(where μ is the dynamic viscosity of the fluid) are the Prandtl number of the fluid, the Schmidt number, magnetic parameter (square of the Hartmann number) and the buoyancy ratio, respectively. Note that by allowing both the wall temperature and concentration to have similar power-law indices, N will always be constant. To eliminate the dependence of M on x, B_0 must be proportional to x to the power $(1+3a)/8$. The transformed boundary conditions become

$$f'(0) = 0, \quad f(0) = f_0, \quad \theta(0) = 1, \quad \phi(0) = 1 \\ f'(\infty) = 0, \quad \theta(\infty) = 0, \quad \phi(\infty) = 0 \tag{13}$$

where $f_0 = (V_w x)/((3+a)(\mathrm{Gr}_x/4)^{1/4})$ is the dimensionless wall mass transfer coefficient such that $f_0 > 0$ indicates suction and $f_0 < 0$ indicates blowing or injection at plate surface. In order to have similar boundary conditions, V_w must be proportional to x to the power $(a-1)/4$.

Of special interest for this flow and heat transfer situation are the skin-friction parameter, average Nusselt number, and the average Sherwood number. These are defined as follows

$$\mathrm{SFP} = \frac{\rho\tau_w L^2}{4\mu^2}\left(\frac{4}{\mathrm{Gr}_L}\right)^{3/4}\left(\frac{L}{x}\right)^2 = f''(0) \tag{14}$$

$$\mathrm{Nu}_{avg} = \frac{hL}{k} = \frac{4}{3}\left(\frac{\mathrm{Gr}_L}{4}\right)^{1/4}\theta'(0) \tag{15}$$

$$\mathrm{Sh}_{avg} = \frac{h_m L}{D} = \frac{4}{3}\left(\frac{\mathrm{Gr}_L}{4}\right)^{1/4}\phi'(0) \tag{16}$$

where τ_w, Gr_L, h and h_m are the shear stress at the wall, Grashof number at $x = L$, average convective heat transfer coefficient and the average mass transfer coefficient, respectively.

3 Numerical method

The implicit finite-difference method discussed by Blottner (1970) is employed in the present work because of its simplicity and its reliable results especially for equations and boundary conditions having forms similar to Eqs. (9)–(13). These equations have been linearized and then descritized using three-point central difference quotients with variable step sizes in the η direction. The resulting equations form a tri-diagonal system of algebraic equations that can be solved by the well known Thomas algorithm (see Blottner, 1970). Due to the nonlinear nature of the equations, an interative solution is required. For convergence, the maximum absolute error between two successive iterations was taken to be 10^{-7}. After many numerical experimentations, a starting step size of 0.001 in the η direction with an increase of 1.015 times the previous step size was found to give accurate results. The total number of points in the η direction was taken to be 399 to ensure proper approach of the solution to the free stream conditions. The method is validated by directly comparing its results with those of Crepeau and Clarksean (1997) for the same problem with all of α, b^*, M, N and V_w are set to zero as shown in Table 1. It is seen from this table that both results are in good agreement. Therefore, this lends confidence in the numerical results to be reported in the next section.

4 Results and discussion

Figures 1 and 2 present the trend of the velocity and the temperature profiles for the cases represented in Table 2 with all of a, b, f_0 and α being set to zero. The increase in Prandtl number reflects a decrease in the thermal diffusion relative to the momentum diffusion. This can be observed from curve II in Fig. 2 compared to curve I, where the temperature for curve II (Pr = 10) is lower than that for

Table 1. Comparison of $-\theta'(0)$ with those of Crepeau and Clarksean (1997) for $\alpha = 0$, $b^* = 0$, $f_0 = 0$, $M = 0$ and $N = 0$

Pr	Crepeau & Clarksean (1997)		Present work	
	$a^* = 0$	$a^* = 1$	$a^* = 0$	$a^* = 1$
0.01	0.08059	−0.8236	0.0600	−0.8413
0.1	0.2302	−0.5425	0.2119	−0.5656
1.0	0.5671	−0.005786	0.5646	−0.005788
10	1.1690	0.7963	1.1720	0.8027
100	2.1910	1.9790	2.1943	1.9835

curve I (Pr = 0.71). Although the velocity decreases as Pr increases as shown in Fig. 1, f' is not a representative quantity for comparing the velocity boundary thickness when the Prandtl number is altered since the dimensional stream function contains one of the parameters of the Prandtl number. The details of the deficiency of the used transformations on velocity boundary-layer thickness when varying the Prandtl number is well explained by Bejan (1993). The presence of a magnetic field in an electrically conducting fluid introduces a force called the Lorentz force which acts against the flow if the magnetic field is applied in the normal direction as considered in the present problem. This type of resistive force tends to slow down the flow. Accordingly, the rate of heat extraction from the wall will reduce resulting in increases in the flow temperature as shown in curve III compared to the reference curve I in both figures. Curve IV shows the effect of internal heat generation when it is a function of the space coordinates on both the velocity and temperature profiles. The value of $a^* = 2.0$ represents a large value of a heat source that causes the temperature of the fluid near the wall to be higher than the wall temperature as shown in curve IV in Fig. 2. Consequently, heat is expected to transfer to the wall. Also, the increased temperature has a direct effect in increasing the thermal buoyancy forces which, in turn, increase the velocity of the flow. Including mass diffusion effects increases the flow velocity and decreases its temperature due to additional concentration buoyancy forces. This is obvious from curves V and VI which correspond to different Lewis numbers compared to curve I in which the concentration buoyancy forces are eliminated by setting N equals to zero.

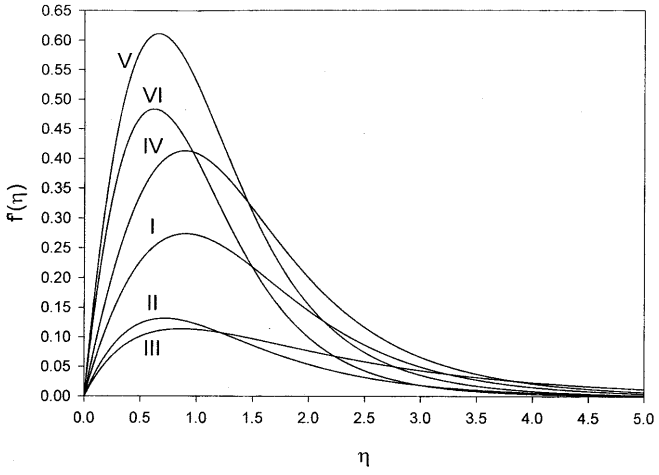

Fig. 1. A Parametric Study on Tangential Velocity Profiles

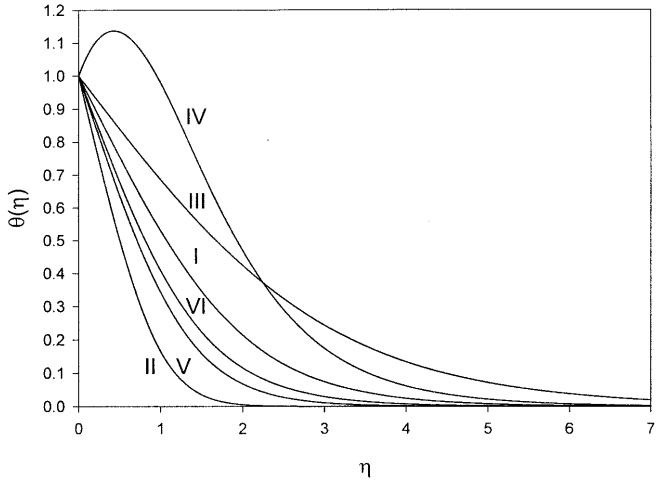

Fig. 2. A Parametric Study on Temperature Profiles

Table 2. Parameteric values for the curves in Figs. 1 and 2

Curve	a^*	M	N	Pr	Sc
I	0	0	0	0.71	0.5
II	0	0	0	10	0.5
III	0	5	0	0.71	0.5
IV	2	0	0	0.71	0.5
V	0	0	3	0.71	0.5
VI	0	0	3	0.71	1.5

Figures 3 and 4 present the effect of the Prandtl number and the power-law index "a" on the skin-friction parameter and the average Nusselt number, respectively. Increases in the values of Pr result in decreases the flow temperature and its absolute slope at the wall. This results in enhancements in the values of the average Nusselt number as shown in Fig. 4. The trend of the skin-friction parameter does represent the actual behavior of the wall shear stress since the latter contains one component of the Prandtl number.

Figures 5–7 show the effects of the square of the Hartmann number M, coefficients of spatial-dependent a^* and temperature-dependent b^* internal heat generation or absorption and the power index "a" on the average Nusselt number, respectively. It is observed from Fig. 2 that as any of M, a^* and possibly b^* increases, the absolute wall temperature slope decreases causing reductions in the values of the average Nusselt number as illustrated in Figs. 5–7, respectively. From Fig. 6, it is noticed that the values of the Nusselt number become negative for large values of a^* and as "a" decreases. This represents the cases where the heat is being transferred to the plate. For positive values of b^* the numerical method does not converge

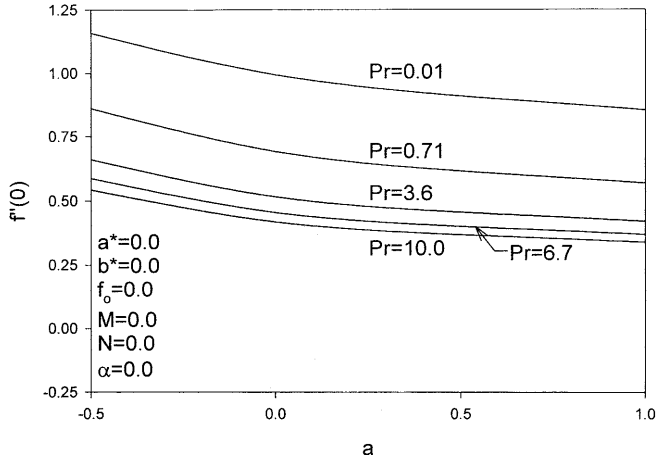

Fig. 3. Effects of Pr and a on the Skin-Friction Parameter

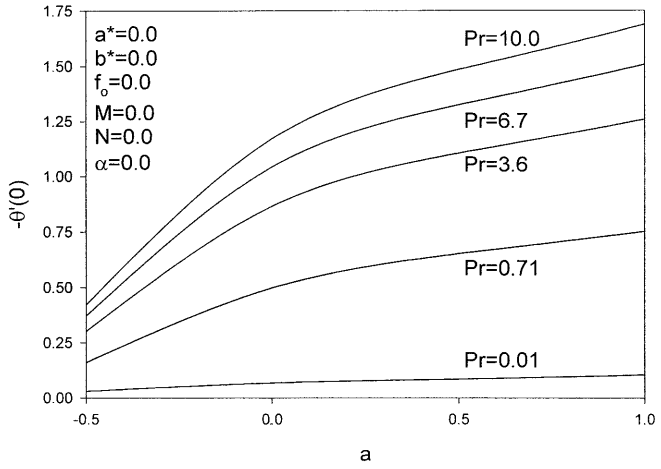

Fig. 4. Effects of Pr and a on the Nusselt Number

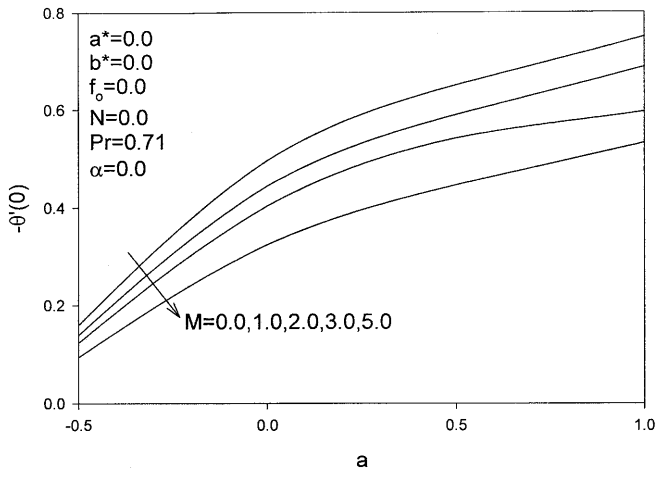

Fig. 5. Effects of M and a on the Nusselt Number

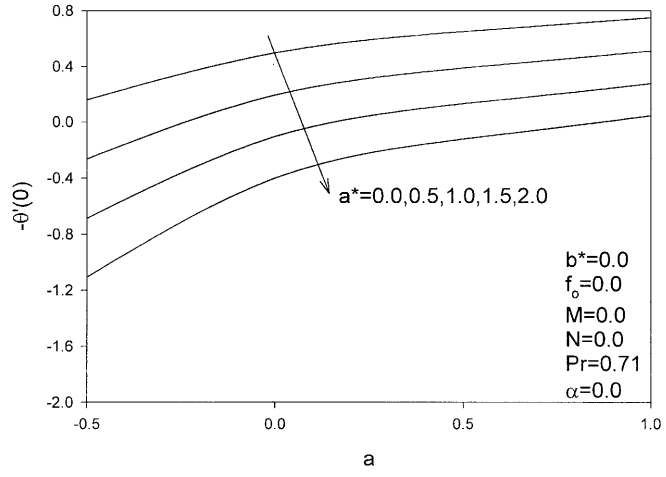

Fig. 6. Effects of a* and a on the Nusselt Number

for the parametric values employed. This indicates that the equations become stiff for this case. For this reason, no results are shown for the case of temperature-dependent heat generation.

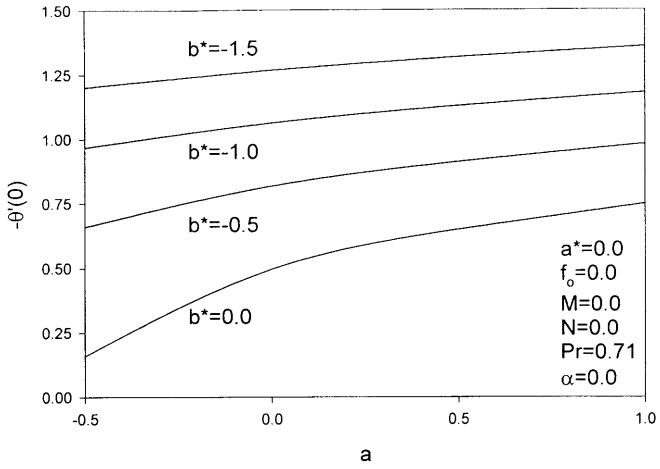

Fig. 7. Effects of b* and a on the Nusselt Number

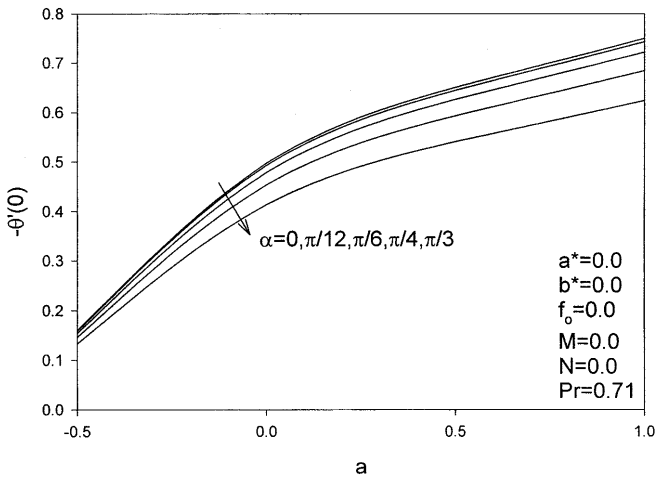

Fig. 8. Effects of α and a on the Nusselt Number

Figure 8 depicts the effect of the inclination angle α from the vertical direction and the power index *a* on the average Nusselt number. As α increases, the buoyancy force in the direction along the plate decreases since the component of *g* in that direction decreases. Hence, the flow velocity which is responsible for convection heat transfer reduces. Accordingly, and as evident from Fig. 8, the average Nusselt number decreases.

Figures 9–12 illustrate the effects of the buoyancy ratio *N* and the Schmidt number Sc on the average Nusselt and Sherwood numbers, respectively. Again, one can notice from Fig. 3 that the absolute wall temperature slope is increased as a result of increasing *N* and decreasing Sc. This causes enhancements in the values of the average Nusselt number and similarly for the average Sherwood number since the energy and concentration equations have the same form. These behaviors can be seen from Figs. 9 and 10. However, increases in the values of Sc cause reductions in the values of the average Nusselt number and increases in the values of the average Sherwood number as shown in Figs. 11 and 12.

In Figs. 13 and 14, the effects of the wall mass transfer coefficient f_0 and the power index "*a*" on the skin-friction

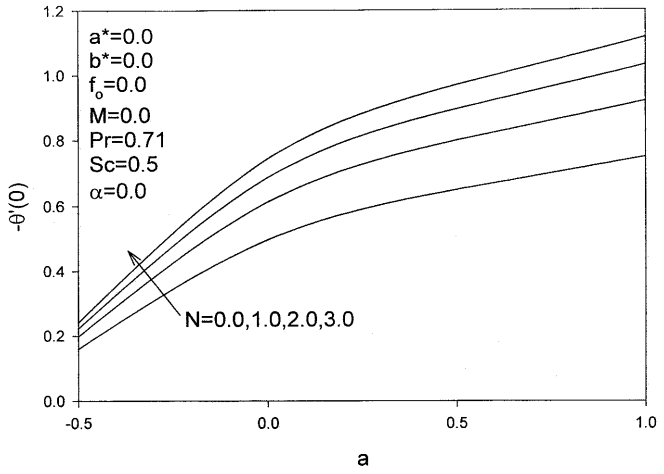

Fig. 9. Effects of N and a on the Nusselt Number

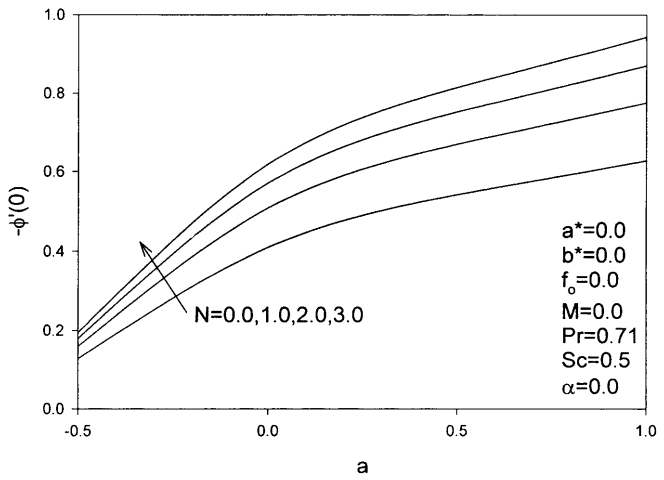

Fig. 10. Effects of N and a on the Sherwood Number

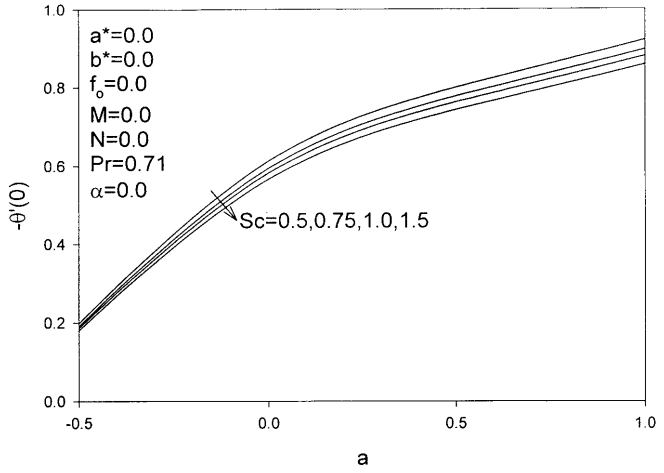

Fig. 11. Effects of Sc and a on the Nusselt Number

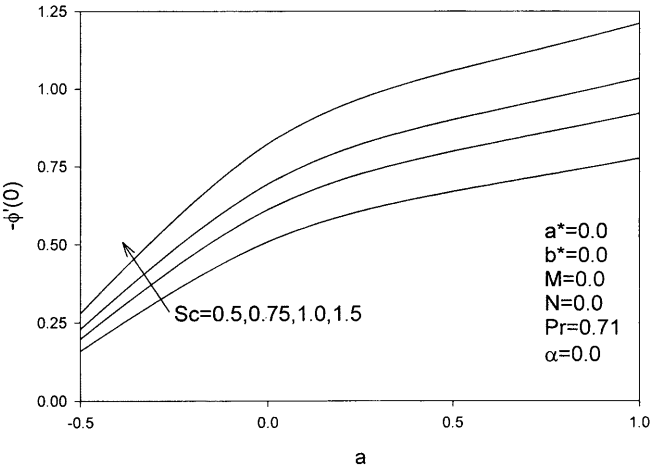

Fig. 12. Effects of Sc and a on the Sherwood Number

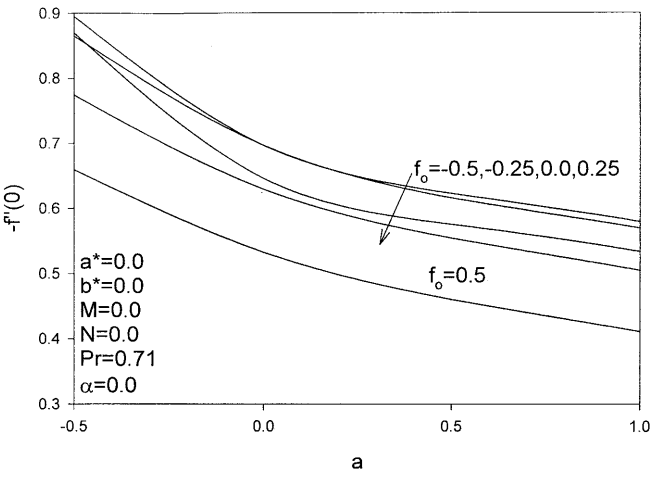

Fig. 13. Effects of f_0 and a on the Skin-Friction Parameter

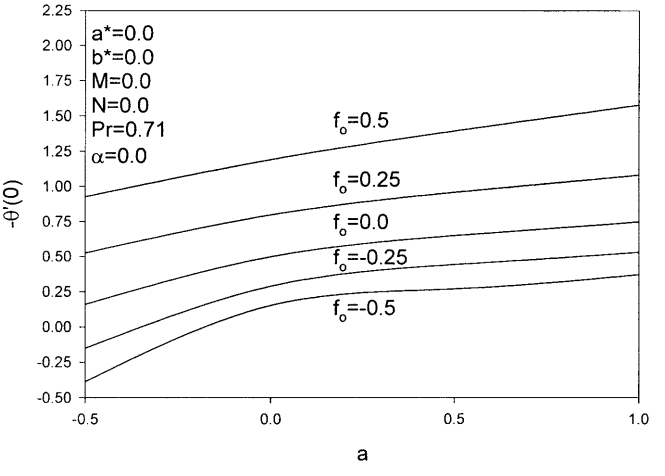

Fig. 14. Effects of f_0 and a on the Nusselt Number

parameter and the average Nusselt number are explained, respectively. Blowing effects when f_0 is less than zero tend to increase the velocity boundary layer. This has the effect of reducing the fluid linear momentum near the wall. Accordingly, the skin-friction parameter and the average Nusselt number decrease as shown in Figs. 13 and 14. In all of the discussed figures, the increase in the power-index "*a*" enhances the wall heat transfer due to the increase in

the wall temperature gradient and decreases the wall shear stresses.

5 Conclusion

The problem of steady, laminar, hydromagnetic heat and mass buoyancy-induced natural convection boundary-layer flow of an electrically-conducting and heat generating or absorbing fluid which is a function of both space and temperature along an inclined permeable plate with power-law variation of both the wall temperature and concentration was considered. The governing equations were developed and transformed using appropriate similarity transformations. The resulting equations were found to be similar for restricted variations of the magnetic field strength and wall normal velocity with the distance along the plate. The transformed equations were then solved numerically by an implicit, iterative, finite-difference scheme. The obtained results for special cases of the problem were compared with previously published work and found to be in good agreement. It was found that while the average Nusselt number decreased as a result of the presence of the magnetic field, it increased due to the imposition of fluid suction at the plate surface. Also, the average Nusselt number was increased due to the presence of space-dependent heat generation effects. Both temperature- and space-dependent heat absorption caused the average Nusselt number to increase. Furthermore, increasing the ratio of the concentration to thermal buoyancies was found to cause enhancements in the values of the average Nusselt number and average Sherwood number. The wall shear stress was found to decrease as a result of wall suction effects and increased values of the power-law index. It is hoped that the present work will serve as a vehicle for understanding more complex problems involving the various physical effects investigated in the present problem.

References

Bejan A (1993) Convection Heat Transfer, 2nd edn., pp 176 Wiley, New York

Blottner FG (1970) Finite-difference methods of solution of the boundary-layer equations. AIAA Journal 8: 193–205

Chamkha AJ (1997a) Hydromagnetic natural convection from an isothermal inclined surface adjacent to a thermally stratified porous medium. Int J Engrng Science 35: 975–986

Chamkha AJ (1997b) Non-darcy fully developed mixed convection in a porous medium channel with heat generation/absorption and hydromagnetic effects. Numer Heat Transfer 32: 853–875

Chen TS; Yuh CF (1980) Combined heat and mass transfer in mixed convection along vertical and inclined plates. Int J Heat Mass Transfer 23: 527–537

Crepeau JC; Clarksean R (1997) Similarity solutions of natural convection with internal heat generation. Journal of Heat Transfer 119: 183–185

Fumizawa M (1980) Natural convection experiment with liquid NaK under transverse magnetic field. J Nuclear Science and Technology 17: 10–17

Gebhart B; Pera L (1971) The nature of vertical natural convection flows resulting from the combined buoyancy effects of thermal and mass diffusion. Int J Heat Mass Transfer 14: 2025–2050

Gray DD (1979) The laminar wall plume in a transverse magnetic field. Int Commun Heat Mass Transfer 22: 1155–1158

Jaluria Y (1980) Natural Convection Heat and Mass Transfer, pp 10–73, Pergamon, New York

Michiyoshi I; Takahashi I; Serizawa A (1976) Natural convection heat transfer from a horizontal cylinder to mercury under magnetic field. Int J Heat Mass Transfer 19: 1021–1029

Moalem D (1976) Steady state heat transfer with porous medium with temperature dependent heat generation. Int J Heat Mass Transfer 19: 529

Pera L; Gebhart B (1972) Natural convection boundary layer flow over horizontal and slightly inclined surfaces. Int J Heat Mass Transfer 16: 1131–1146

Sparrw EM; Cess RD (1961) Temperature dependent heat sources or sinks in a stagnation point flow. Appl Sci Res A10: 185

Vajravelu K; Nayfeh J (1992) Hydromagnetic convection at a cone and a wedge. Int Commun Heat Mass Transfer 19: 701–710

Vajravelu K; Hadjinicolaou A (1993) Heat transfer in a viscous fluid over a stretching sheet with viscous dissipation and internal heat generation. Int Commun Heat Mass Transfer 20: 417–430

Westphal BR; Keiser DD; Rigg RH; Lang DV (1994) Production of metal waste forms from spent nuclear fuel treatment, DOE Spent Nuclear Fuel Conference, Salt Lake City, UT, pp 228–294